ELSEVIER

Ultramicroscopy 54 (1994) 116–124

ultramicroscopy

Scanning tunneling microscopic studies of surface reconstructed structures for metal/Si(100) systems

T. Ichinokawa [a], H. Itoh [a], A. Schmid [a], D. Winau [a], J. Kirschner [b]

[a] *Department of Applied Physics, Waseda University, 3-4-1 Ohkubo, Shinjuku-ku, Tokyo 169, Japan*
[b] *Max-Planck-Institut für Mikrostrukturphysik, Weinberg 2, O-4050 Halle / Saale, Germany*

Received 31 August 1993; accepted 10 September 1993

Abstract

Growth modes and surface reconstructions in the systems of Group I–V and transition metals of the Periodic Table on Si(100) have been studied by scanning tunneling microscopy (STM) as a function of coverage and substrate temperature. The adsorption sites of metal, formation of superstructures and growth mode as functions of coverage and temperature are classified briefly depending on the type of metal. The mechanisms of epitaxial growth and reconstruction are discussed based on the phase diagrams of these systems.

1. Introduction

The surface structures and growth modes in metal–semiconductor interfaces have been investigated to make clear the formation mechanisms of superstructures as functions of the type of metal, substrate structure, metal coverage and deposition temperature. A number of studies by low energy electron diffraction (LEED) and Auger electron spectroscopy (AES) found that there are many superstructures depending on the coverage and deposition temperature. However, structures determined by these methods are given only by symmetries and lattice constants and not by atomic arrangements. Therefore, the formation mechanisms of superstructures related to the growth mode have not been cleared on an atomic scale.

Particularly, the data for the metal/Si(100) systems are a few comparing to those for metal/Si(111) systems in spite of the simple atomic structure of the substrate surface. Thus, we planned to study the surface structures and growth modes on an atomic scale using scanning tunneling microscopy (STM) for various metals on the Si(100)$2 \times n$ surface to understand the reconstruction mechanism as functions of the type of metal, coverage and deposition temperature. The different adsorption sites, growth modes and formation mechanisms of superstructures depending on temperature are classified by the type of metal. Typical formation mechanisms of superstructures and several modes of epitaxial growth are presented for the metal/Si(100) systems on an atomic scale based on their phase diagrams.

2. Experimental

Ag (Group I), Mg (Group II), Al (Group III), Pb (Group IV) and Pt, Pd (transition metals) on Si(100)2×1 systems were prepared in ultra-high vacuum (UHV) of 2×10^{-10} Torr and the struc-

SSDI 0304-3991(94)00025-I

tures of deposited surfaces were studied by LEED, AES and UHV-STM (OMICRON UHV-STM) as a function of coverage and substrate temperature. The substrate temperature was elevated by electron beam bombardment from the back side of the specimen and measured by an infrared pyrometer or a thermocouple. All STM images were taken at room temperature after the sample was transferred from the sample holder of LEED and AES to that of STM, by an oblique-stick. The coverages are measured by a quartz thickness monitor and given in monolayers, with 1 ML defined as the Si atom density on the Si(100) surface (1 ML = 6.8×10^{14} atoms/cm^2). The local coverage was also estimated by counting the density of metal-related features on the surface seen in the STM images.

3. Results and discussion

3.1. Adsorption sites and first layer structures deposited at room temperature

3.1.1. Adsorption sites

For adsorption of metals on the Si(100)2×1 structure, there are five sites as shown in Fig. 1 [1]. According to our STM observations for metal/Si(100) systems, the most stable site is T3 in the hollow site between adjacent Si dimer rows surrounded by four Si dimers. However, the difference in bonding energy between T3 and T4 is small and depends on the number of valence bonds of the metal atom. An adsorption unit is not only an atom, but also a dimer. Fig. 2 shows STM images of the adsorption sites for Ag at low coverage [2]. The adsorption site is T4 and an Ag chain consists of orthogonal dimers.

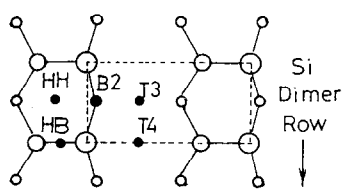

Fig. 1. Top view of the Si(100)2×1 surface with asymmetric dimers. The 2×1 unit cell is indicated by dashed lines. The five adsorption sites, HH, HB, T3, T4 and B2 are indicated.

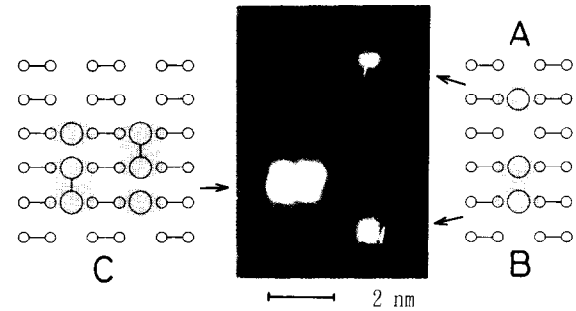

Fig. 2. Different Ag adsorption configurations in the grooves between the vertical Si dimer rows. The Ag structures are brighter than the Si dimers. (A) Single Ag atom in the bridge site between two Si dimers of adjacent rows, (B) Ag dimer and (C) two small Ag chains each consisting of three Ag atoms.

For alkali-metal adsorption of Cs, Na and K on Si(100), a double-layer model aligned on the T3 and HH sites has been proposed by Abukawa, Okane and Kono for the first layer [3]. Moreover, for the Pt/Si(100) and Pd/Si(100) systems, metal atoms are embeded at the HH site of Levine's model [4] at high temperature after the reconstruction and form a regular superstructure of c(4 × 2) [5,6]. The optimized configurations and electronic structures of the first layer before and after reconstructions in the metal/Si(100) systems are particularly interesting from the theoretical viewpoint.

3.1.2. Surface structures of the first layer deposited at room temperature

3.1.2.1. Monolayer growth. Most metals used in the present experiment form ad-atom lines perpendicular to the underlying Si dimer rows. These metal (Al, Pb and Mg) lines form the two-dimensional (2D) islands and the islands cover all the surface with increasing coverage. For Al, ad-dimers grow in a long line perpendicular to the Si dimer rows below 300°C and the interline spacing decreases with increasing coverage [7]. The growth pattern varies depending on the deposition temperature. A completed layer of ad-dimer lines has a 2×2 structure without destruction of the underlying Si dimer structure. However, whether the metal lines consist of single atoms or dimers

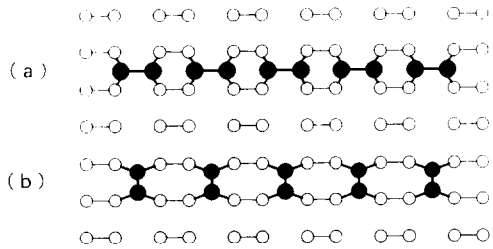

Fig. 3. Two possible atomic arrangements of the ad-dimer line; (a) is a parallel and (b) an orthogonal ad-dimer structure.

depends on the type of metal. For the dimer lines, there are two types of dimer orientations against dimerization of the underlying Si dimers, e.g., parallel and orthogonal dimer configurations as shown in Fig. 3.

From our STM observations, Mg [8] and Pb [9] form single atom lines and the first layer of the 2×2 structure is completed at 0.25 ML, whereas Al and Ag form dimer lines and the first layer of 2×2 is completed at 0.5 ML. Furthermore, the Al dimer line [7] has a parallel dimer configuration contrary to the orthogonal dimer structure in the homoepitaxial growth of C, Si and Ge. Here, it should be noticed that the structure of the first layer is not always perfect: e.g., Ag dimer rows grown parallel to the Si dimer rows are mixed with perpendicular Ag dimer lines and 3D islands begin to grow before the completion of the first layer in Ag.

For Pb or Ag deposition at room temperature, different structures of $c(4 \times 8)$ and $c(4 \times 2)$ are observed mixed with the 2×2 structure as shown in Fig. 4 for Pb [9,2]. These structures are formed correlating with the buckling of the underlying Si dimer rows, because the adsorption of metals stabilizes the buckling between adjacent Si dimer rows in phase or out of phase. For Pb deposition, 3D islands grow after the formation of 2nd and 3rd layers of the structures of 2×1 and $c(4 \times 4)$ [9] and the growth mode is a modified type of Stranski–Krastanov [S-K]. The different growth modes depending on the type of metal will be described later as a parameter of the deposition temperature.

3.1.2.2. Island growth. For depositions of Pt [3] and Pd [4] at room temperature, small clusters of nm size nucleate in the Volmer–Weber (V-W) mode and the dimer structure of Si(100) 2×1 is simultaneously observed by STM with clusters as shown in Fig. 5 [4]. At a coverage of several monolayers, all of the surface is covered by clusters. As a result, the LEED pattern of the Si(100) 2×1 structure becomes obscure with increasing coverage and disappears at a coverage of several monolayers. These facts indicate that interaction between Si and metal is weakest for Pt and Pd, intermediate for Ag and Pb and becomes stronger in sequence of Mg and Al.

3.2. Reconstructed structure at high temperature

The structures of deposited surfaces other than Pb change into other structures at the reconstruction temperatures at coverage less than 1 ML. So far a number of the reconstructed structures were observed by LEED above the critical temperatures as shown in Fig. 6 by an example of the Al/Si(100) phase diagram. The formation mechanisms of the reconstructed structures are different depending on the type of metal and can be classified briefly into the following three types.

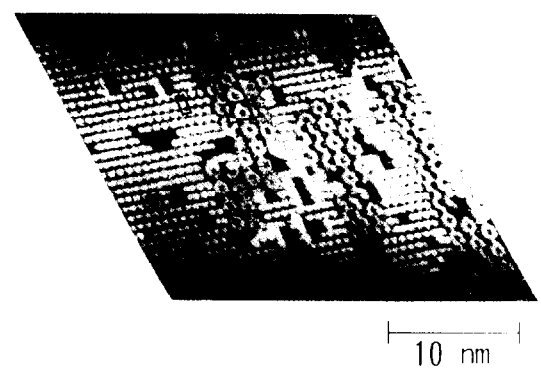

Fig. 4. STM image of a mixed structure of 2×4 and $c(4 \times 8)$ for the Pb-deposited surface of 0.2–0.7 ML at room temperature. The structure of hexagonal subunits with a $c(4 \times 8)$ symmetry are mixed with a regular arrangement of the 2×4 symmetry. The $c(4 \times 8)$ structure is formed by out-of-phase buckling between adjacent Si dimer rows.

3.2.1. Combination with Si missing dimer defects

The clusters of Si missing dimer defects lying on the clean Si(100) surface disperse into the individual Si missing dimer defects by adsorption of metal atoms at high temperature and single Si missing dimer defects of each combined with an adsorbed metal atom form a superstructure by long range order. For instance, Pt and Pd [3,4] produce a superstructure of c(4 × 6) above 700°C at a coverage between 1/6 and 1/3 ML, as shown in Fig. 7. The reconstructed structure formed at high temperature covers all the surface and is stable from room temperature to the desorption temperature after the reconstruction. Above reconstruction coverages, 3D islands nucleate on the reconstructed structure by the S-K mode and the islands are usually composed of silicides by reacting with the Si substrate.

A reconstruction similar to that of Pt and Pd was also reported in a Ni-contaminated surface of Si(100)2 × n. The superstructure of the Si missing dimer defects induced by a Ni impurity, i.e., the 2 × n structure ($6 < n < 10$), has been observed depending on Ni coverage on the surface.

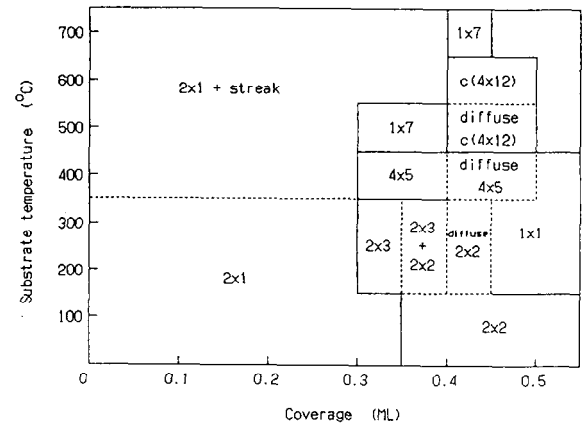

Fig. 6. Formation diagram of surface structures for the Al/Si(100) system at coverages less than 1 ML and at substrate temperatures from room temperature up to 700°C.

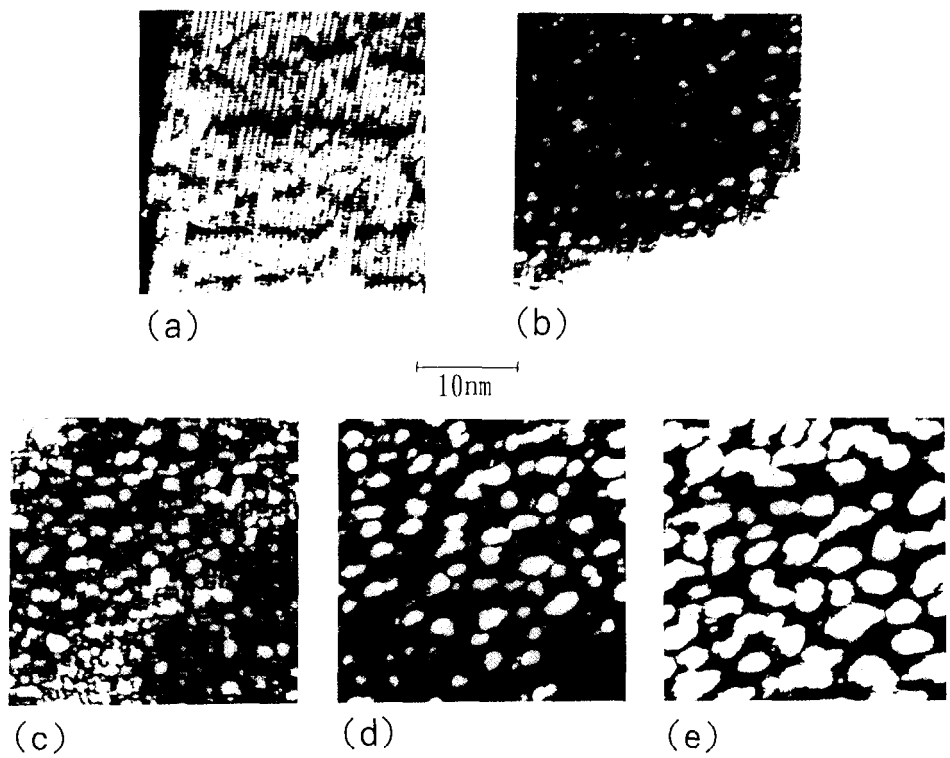

Fig. 5. STM images of Pd-deposited surface at room temperature at various coverages: (a) 0.02, (b) 0.04, (c) 0.3, (d) 1.2 and (e) 2.4 ML.

The analyses of this phase were performed by LEED [10,11] and STM [12].

3.2.2. Long range ordering of molecular clusters consisting of several metal atoms

The adsorbed metal atoms form molecular clusters each consisting of several atoms at high temperature; a molecular cluster buckles underlying Si dimer rows in the anti-phase or in-phase mode for adjacent Si dimer rows. The long range ordering of molecular clusters forms superstructures caused by buckling of the Si dimer rows.

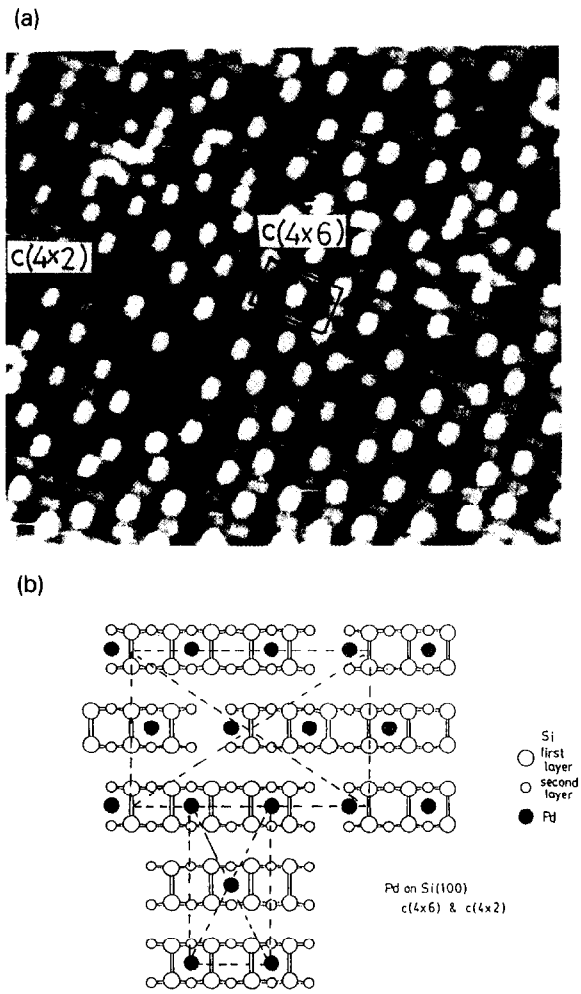

Fig. 7. (a) STM image of the $c(4\times2)+c(4\times6)$ surface and (b) model of $c(4\times2)+c(4\times6)$. $c(4\times2)$ is composed of a subunit which consists of two dimers and a Pd atom embedded at the center, and $c(4\times6)$ consists of a subunit in which a Si dimer is missing from the $c(4\times2)$ subunit.

For an Al-deposited surface above 500°C, the $c(4\times2n)$ structure begins to form at 0.18 ML as illustrated by Fig. 8 [13]. It is a stable structure from room temperature to desorption temperature. The $c(4\times2n)$ structure is formed in agreement with the buckling of Si dimer rows and covers all the surface at approximately 0.25 ML. The structure model of $c(4\times12)$ is shown in Fig. 9 for $n=6$. Above the reconstruction coverage, the second layer islands composed of Al and Si are observed on the reconstructed surface of $c(4\times12)$ by displacement of Si atoms from the substrate to the top of the surface as shown in Fig. 8.

A reconstruction mechanism similar to that of Al was reported for the Group III metals In and Ga on Si(100) 2×1 systems by Baski et al. [14,15] and for a Ni-contaminated surface of $\sqrt{19}\times\sqrt{19}$ on Si(111) by Wilson and Chiang [16].

3.2.3. Superstructure formation due to the optimized configuration between metal and Si layers

For most metals, superstructures formed at low temperature transform irreversibly into reconstructed structures at the reconstruction temperatures without any relationship to the Si missing dimer defects or the formation of molecular clusters as described in the previous sections. In this case, the superstructure transformation is caused by an irreversible change from low to high temperature phase which is determined by an optimized configuration between metal and Si layers.

For instance, Ag forms a 2×3 structure as shown in Fig. 10 above 500°C [2] and Mg forms 2×3 and 2×2 structures depending on the coverage above 300°C [8]. Furthermore, Pb forms first, second and third layers of $c(4\times8)$, 2×1 and $c(4\times4)$ structures, respectively, depending on coverage above room temperature. These structures are formed by minimization of total energy for chemisorbed states of metal on Si(100) as a function of metal coverage.

Above the reconstruction temperature, most metals grow in the S-K mode on the reconstructed surface. However, 3D islands of Pb grow

in the S-K mode after the formation of 2nd and 3rd layers of 2×1 and $c(4 \times 4)$. It should be noticed that growth modes depend on the type of metal and deposition temperature and then there are a number of modifications for the S-K mode.

3.3. Step structure transformation induced by metal adsorption at high temperature

Vicinal Si(100) surfaces are well known to form single and double steps depending on the miscut angle and annealing temperature. Recently, we found that the transformation from double steps to quadruple steps is induced by Ag adsorption at 500°C for the Si(100)2×1 double-stepped surface of miscut angle 4° [17]. The structure of the Ag/Si(100) surface changes at 500°C from 2×2 to 2×3 at an Ag coverage of 0.3 ML [2]. The step structure changes simultaneously with the surface structure change. Fig. 11 shows STM images taken before and after the step structure transformation. The step height and the terrace width become twice as large as shown in Fig. 12 by a line scan and the spacing between protrusion rows perpendicular to the step edge in the direction of the step edge changes from two-to threefold. The LEED patterns also show that the two-fold axis of the clean surface is switched from the direction parallel to the step edge to the perpendicular direction caused by the reconstruction. This fact indicates that D_B steps change into Q_A steps by the surface reconstruction and then

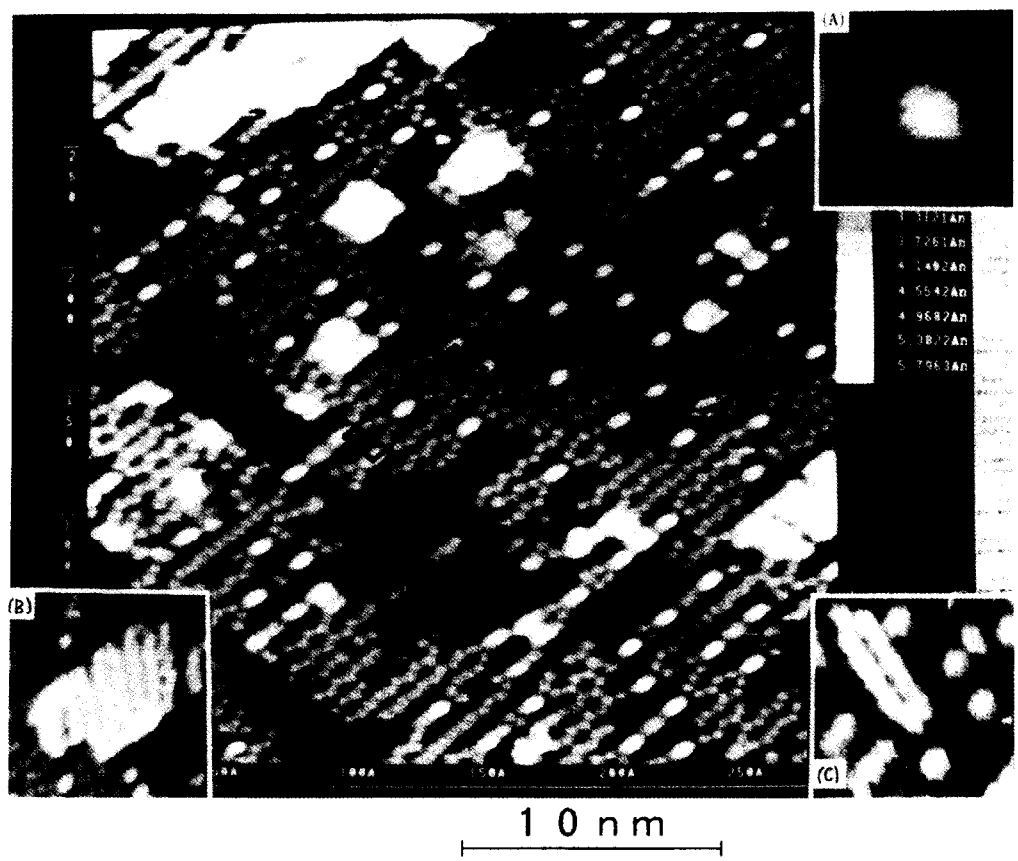

Fig. 8. STM image of Al-deposited surface of 0.16 ML at 500°C. The bright protrusions begin to form $c(4 \times 2n)$ as shown by the rectangle. The magnified image of a molecular cluster has hexagonal symmetry as shown in insert (A). Two types of layer islands with structures of 1×2 and 2×2 are Si and Al formed in the second layer as shown in inserts (B) and (C), respectively.

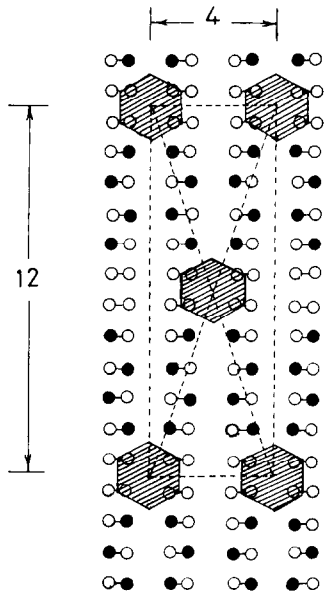

Fig. 9. Model of the structure of Al/Si(100)c(4×12).

the three-fold axis of the 2 × 3 structure is parallel to the step edge. The transformation dynamics will be interpreted as shown in Fig. 13 by the fact that the topmost layers of every second terrace slip down to the next lower terraces and the

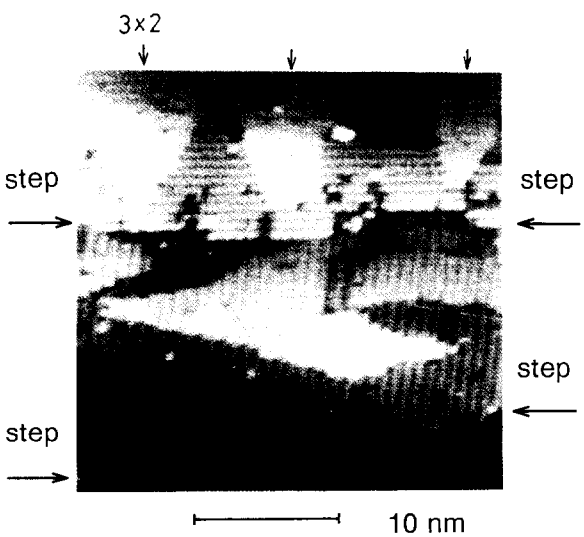

Fig. 10. STM image of the growth of Ag/Si(100)2×3. The 2×3 structure covers all the surface at a coverage of approximately 0.3 ML.

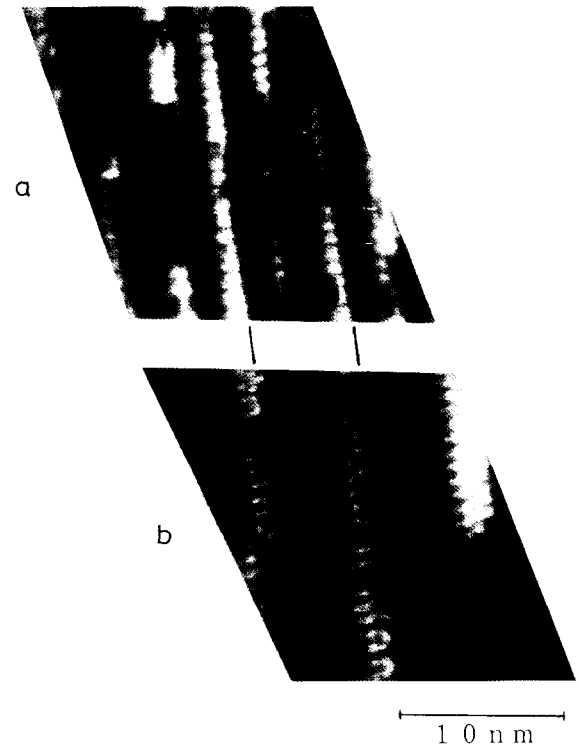

Fig. 11. (a) STM image of the clean stepped surface and (b) that of the surface covered by 0.3 ML Ag at 500°C. The terrace width of 3.5 nm is doubled to 7.0 nm by the surface structure change, as indicated by the bars. The Si dimer rows with an inter-row spacing of $2a$ change to the protrusion rows with an inter-row spacing of $3a$. Image (a) was taken at bias −3.0 V and tunneling current 0.1 nA and (b) at +1.9 V and tunneling current 0.05 nA.

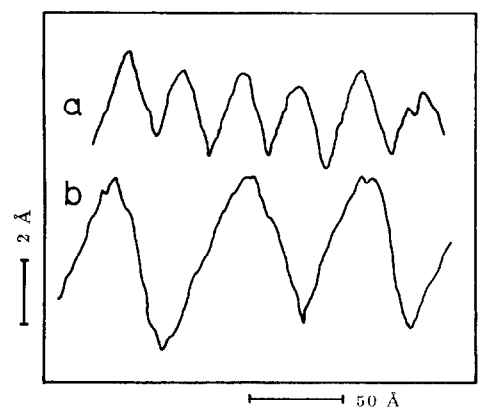

Fig. 12. Line profile perpendicular to the step edge, (a) Si(100)2×1 vicinal surface (b) Ag-covered stepped surface. The terrace width and step height of (b) are twice those of (a) and the steps in (b) are quadruple steps.

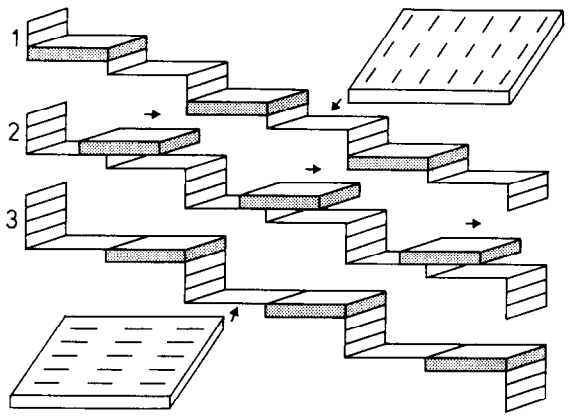

Fig. 13. Diagram illustrating the step structure change on the Si(100) single domain surface induced by Ag adsorption at 500°C. The topmost layers of every second terrace slip down to the next lower terraces and the direction of Si dimer rows rotates 90° by the transformation. The terrace width and step height become twice as large by this model.

appearing terrace exhibits a 90° rotated top layer structure with Si(100)-Ag 2×3.

On the vicinal Si(100) clean surface, the D_B steps are stable due to the tensile stress perpendicular to the Si dimer rows, whereas the Q_A steps are the most stable in the Ag-covered stepped 2×3 surface. This fact is due to the relaxation of the anisotropic surface stress caused by the adsorption of Ag atoms in the grooves between adjacent Si dimer rows.

Thus, the step energy changes completely by Ag adsorption and the Q_A steps are the most stable step structure on the Ag-covered stepped 2×3 surface. The quantitative explanation should be carried out by theoretical calculations for the step energies depending on the surface structure.

4. Conclusion

The growth modes of metals on the Si(100)2×1 surface are almost similar within the same Group, but the valence bond features of metals in the same Group change gradually with increasing atomic number. Therefore, the growth mode varies with atomic number even in the same Group. The adsorption sites and the optimized structures of metal/Si(100) surfaces at low and high temperatures have been investigated by STM for several metals. The atomic arrangements observed by STM provide information on the stable structure in the physisorbed and chemisorbed states and suggest different mechanisms of reconstruction for the metal/Si(100) systems.

The modifications of growth mode are caused by the local structure defects and the mixture of local different phases and growth. The growth and reconstructed structures of metals on Si surfaces are very complicated depending on the type of metal and deposition temperature. Moreover, the step structure transformation induced by the surface reconstruction was observed at 500°C in the Ag-adsorbed vicinal surface of Si(100) with single domain. Quantitative analyses should be performed with the help of theoretical calculations.

Acknowledgement

The present work was supported by a Grant-in-Aid for Scientific Research and Culture from the Japanese Ministry of Education.

References

[1] Y. Morikawa, K. Kobayashi and K. Terakura, Surf. Sci. 283 (1993) 377.
[2] D. Winau, H. Itoh, A.K. Schmid and T. Ichinokawa, Surf. Sci. 303 (1994) 139.
[3] T. Abukawa, T. Okane and S. Kono, Surf. Sci. 256 (1991) 370.
[4] J.D. Levine, Surf. Sci. 34 (1973) 90.
[5] H. Itoh, S. Narui, A. Sagawa and T. Ichinokawa, Phys. Rev. B 45 (1992) 11136.
[6] H. Itoh, S. Narui, H. Tanabe and T. Ichinokawa, Surf. Sci. 284 (1993) 236.
[7] H. Itoh, J. Itoh, A. Schmid and T. Ichinokawa, Phys. Rev. B 48 (1993) 14663.
[8] Y. Kawashima, H. Tanabe, H. Itoh and T. Ichinokawa, Surf. Sci. (1994) submitted.
[9] H. Itoh, H. Tanabe, D. Winau, A. Schmid and T. Ichinokawa, STM'93 Conf., Beijing, 1993, submitted.
[10] K. Kato, T. Ide, S. Miura, A. Tanabe and T. Ichinokawa, Surf. Sci. 194 (1988) L87.
[11] J.A. Martin, D.E. Savage, W. Moritz and M.G. Lagally, Phys. Rev. Lett. 56 (1986) 1936.
[12] H. Niehus, U.K. Köhler, M. Copel and J.E. Demuth, in:

Proc. 3rd Int. Conf. on STM, Oxford, 1988, Vol. 23, Suppl. 3 (Royal Microscopical Society, London, 1989) p. 13.
[13] H. Itoh, J. Itoh, A. Schmid and T. Ichinokawa, Surf. Sci. 302 (1994) 295.
[14] A.A. Baski, J. Nogami and C.F. Quate, J. Vac. Sci. Technol. A 9 (1991) 1946.
[15] A.A. Baski, J. Nogami and C.F. Quate, Phys. Rev. B 43 (1991) 9316.
[16] R.J. Wilson and S. Chiang, Phys. Rev. Lett. 58 (1987) 2575.
[17] D. Winau, H. Itoh, A. Schmid and T. Ichinokawa, Phys. Rev. B (1994) submitted.